Christiane Stoll, Markus Seibald and Hubert Huppertz*

Synthesis and characterization of $K_5Sn_2OF_{11}$

https://doi.org/10.1515/znb-2019-0158
Received September 30, 2019; accepted October 20, 2019

Abstract: The potassium oxidofluoridostannate(IV) fluoride $K_5Sn_2OF_{11}$ was synthesized *via* a solid-state route at $T = 300$°C in arc-weldeded copper ampoules. It crystallizes in the orthorhombic system in the acentric space group *Ama2* (no. 40) with a unit cell volume of $V = 2.5727(4)$ nm^3. The cell parameters are $a = 1758.3(2)$, $b = 2452.3(2)$ and $c = 596.7(1)$ pm. As a main structural motif, $K_5Sn_2OF_{11}$ exhibits two different kinds of dinuclear $[Sn_2OF_{11}]^{5-}$ units, which are embedded into a matrix consisting of potassium cations and fluoride anions. The substance was characterized by single-crystal and powder X-ray diffraction, as well as by FT-IR spectroscopy.

Keywords: crystal structure; FT-IR spectroscopy; potassium oxidofluoridostannate(IV) fluoride.

Dedicated to: Professor Arndt Simon on the occasion of his 80th birthday.

1 Introduction

Oxidofluoridometallates are a fascinating class of compounds with a wide variety of structural motifs, ranging from tetrahedral, pentahedral and octahedral complex units to hepta-, octa- and nona-coordinated anions [1]. Octahedra are the most commonly observed units, whether in isolated or condensed format [1]. As a consequence, the structural motifs range from 0-dimensional (quasi-isolated) units to 3-dimensional networks [1]. Octahedral units like $[MoOF_5]^-$ in K_3MoOF_7 [2], corner-sharing units like $[Eu_2O_{10}F]^{5-}$ in $K_5Eu_2FSi_4O_{13}$ [3], and edge-sharing building blocks like $[Ti_2O_8F_2]^{10-}$ in $Ba_2Ti_2Si_2O_9F_2$ are observed [4]. These units have a finite length. Even though a large number of transition metal oxidofluorides are known, just a few oxyfluoride compounds of main group elements have been characterized based on single-crystal data. Within this group, compounds incorporating tin as their central cation are scarcely mentioned. Crystal structures of oxidofluoridostannates show 0-dimensional quasi-isolated anions, layers of edge- and corner-sharing octahedra, and 3-dimensional networks with bridging oxygen and fluorine atoms [5–7]. A complex 3-dimensional motif has been observed within the structure of Sn_4OF_6. The network consists of $[Sn_3OF_3]^-$ anions arranged in columns, which are additionally interconnected by $[Sn_2F_6]^{2+}$ cations [5]. A 2-dimensional motif has been observed in $Sn_4O_2F_{10}$. Within this structure, tin is octahedrally coordinated by both oxygen and fluorine atoms. These octahedra are interconnected in $[Sn_3O_2F_{10}]^{2-}$ units, which are assembled in layers [6]. The dimeric quasi-isolated $[Sn_2O_2F_4]^{2-}$ motif was discovered in the form of edge-sharing bipyramids in $[Sn_2O_2F_4]Sn_2$ [5, 7]. Few other reports refer to tin oxyfluoride compounds. For example, Kolditz and Preiss reported on $K_4Sn_2OF_{10}$ in 1963 [8]. They proposed a dinuclear $[Sn_2OF_{11}]^{5-}$ anion with a bridging oxygen atom as the structural unit for this compound, but a crystal structure analysis had not been carried out [8].

Within this contribution, we report on $K_5Sn_2OF_{11}$, a potassium oxidofluoridostannate(IV) fluoride exhibiting two different kinds of quasi-isolated dinuclear $[Sn_2OF_{11}]^{5-}$ units with oxygen as the bridging atom.

2 Experimental section

2.1 Synthesis

$K_5Sn_2OF_{11}$ was synthesized *via* a solid-state reaction carried out in closed copper ampoules. KHF_2 (Alfa Aesar, Haverhill, USA, 99+%) and SnO_2 (Strem Chemicals, Newburyport, USA, 99.9%) with a molar ratio of 2:1 were weighed in and ground together under inert gas atmosphere in a glove box (MBraun Inertgas-System GmbH, Germany). The as prepared mixture was subsequently transferred into a copper ampoule, which was sealed in a miniaturized arc-welding equipment [9]. The ampoule was placed into a silica tube (400 mbar argon) and positioned into a tube furnace and heated at a rate of 3 K min^{-1} to a temperature of 300°C, held for 96 h, and cooled down to 250°C with a rate of 0.1 K min^{-1}. At this

***Corresponding author: Hubert Huppertz,** Institut für Allgemeine, Anorganische und Theoretische Chemie, Universität Innsbruck, Innrain 80–82, 6020 Innsbruck, Austria,
e-mail: hubert.huppertz@uibk.ac.at
Christiane Stoll: Institut für Allgemeine, Anorganische und Theoretische Chemie, Universität Innsbruck, Innrain 80–82, 6020 Innsbruck, Austria
Markus Seibald: OSRAM Opto Semiconductors GmbH, Mittelstetter Weg 2, 86830 Schwabmünchen, Germany

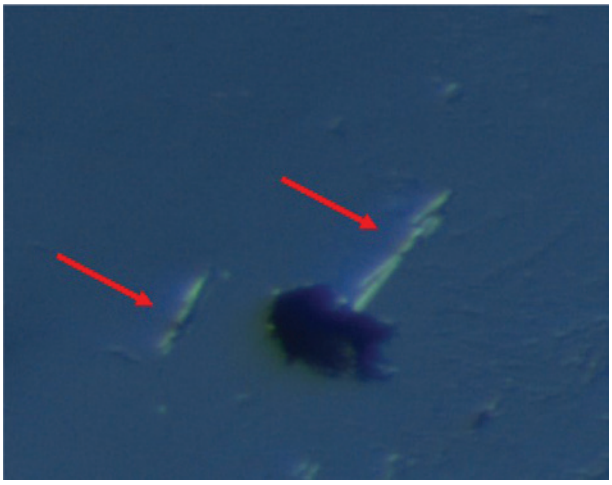

Fig. 1: Needle-shaped crystals of $K_5Sn_2OF_{11}$ (indicated by red arrows) viewed through a polarization microscope.

Table 1: Crystal data and structure refinement of $K_5Sn_2OF_{11}$.

Empirical formula	**$K_5Sn_2OF_{11}$**
Molar mass, g mol^{-1}	657.88
Crystal system	Orthorhombic
Space group	*Ama*2 (no. 40)
Powder data	
Powder diffractometer	Stoe Stadi P
Radiation; λ, pm	Mo$K\alpha_1$; 70.93
Temperature, K	293(2)
a, pm	1764.7(5)
b, pm	2458.3(7)
c, pm	600.4(2)
V, nm^3	2.605(2)
Single-crystal data	
Single-crystal diffractometer	Bruker D8 Quest Photon 100
Radiation; λ, pm	Mo$K\alpha$; 71.07
a, pm	1758.3(2)
b, pm	2452.3(2)
c, pm	596.7(1)
V, nm^3	2.5727(4)
Formula units per cell, *Z*	8
Calculated density, g cm^{-3}	3.40
Temperature, K	183(2)
Absorption coefficient, mm^{-1}	5.6
F(000), *e*	2416
2θ range, deg	4.6–60.0
Range in *hkl*	±22, ±31, ±7
Total no. of reflections	48348
Independent reflections/ref. parameters/R_{int}	3051/184/0.0804
Reflections with $I > 2\,\sigma(I)$	2759
Goodness-of fit on F_i^2	1.123
Absorption correction	Semi-empirical (from equivalents)
Final *R*1/*wR*2 ($I > 2\sigma(I)$)	0.0314/0.0431
Final *R*1/*wR*2 (all data)	0.0389/0.0443
Largest diff. peak/hole, e Å^{-3}	0.93/ −1.04
BASF	0.31(4)/0.69(4)

temperature, the sample was annealed for another 24 h. Finally, the sample was cooled down to 100°C with a rate of 0.1 K min^{-1}, followed by quenching to room temperature. A colorless sample was obtained as needle-shaped crystals (Fig. 1).

2.2 X-ray structure determination

Analysis of the powder sample was carried out using a STOE Stadi P powder diffractometer. A molybdenum radiation source Mo$K\alpha_1$ ($\lambda = 70.93$ pm) in combination with a Ge(111) primary beam monochromator and a Mythen 2 DCS4 detector enabled the detection of the diffraction data. Measurements were taken within the 2θ range of 2.0–40.4° with a step size of 0.015°.

Single-crystal analysis was carried out on a needle-shaped crystal. The sample was covered with perfluoropolyalkylether and a crystal was isolated with the help of a polarization microscope. For the collection of the intensity data, a Bruker D8 Quest diffractometer (Bruker, Billerica, USA) was used. It is equipped with a Photon

Table 2: Wyckoff positions, atomic coordinates, and equivalent isotropic displacement parameters U_{eq} (Å^2) of $K_5Sn_2OF_{11}$.

Atom	**Wyckoff position**	***x***	***y***	***z***	U_{eq}
Sn1	8*c*	0.07798(2)	0.04528(2)	0.1378(2)	0.0081(1)
Sn2	8*c*	0.14523(2)	0.28975(2)	0.1220(2)	0.0087(1)
K1	8*c*	0.0914(1)	0.44303(7)	0.1791(3)	0.0225(5)
K2	8*c*	0.10286(7)	0.14492(5)	0.6256(5)	0.0122(3)
K3	8*c*	0.52856(8)	0.19893(6)	0.1262(5)	0.0185(3)
K4	4*b*	¼	0.1564(1)	0.0829(5)	0.0238(8)
K5	4*b*	¼	0.25727(8)	0.6203(6)	0.0139(5)
K6	4*b*	¼	0.4136(2)	0.6871(5)	0.0242(8)
K7	4*b*	¼	0.5398(1)	0.0649(4)	0.0121(5)
F1	8*c*	0.0255(3)	0.0608(2)	0.4226(8)	0.026(2)
F2	8*c*	0.0334(2)	0.3050(2)	0.111(2)	0.020(1)
F3	8*c*	0.0334(3)	0.6116(2)	0.4993(9)	0.028(2)
F4	8*c*	0.1173(4)	0.2359(3)	0.3599(9)	0.021(2)
F5	8*c*	0.1414(3)	0.5403(2)	0.3648(8)	0.020(2)
F6	8*c*	0.1561(5)	0.3471(4)	0.352(2)	0.047(2)
F7	8*c*	0.1567(3)	0.0932(2)	0.2648(8)	0.022(2)
F8	8*c*	0.6189(4)	0.2680(3)	0.3979(9)	0.018(2)
F9	8*c*	0.6371(3)	0.0141(2)	0.2779(9)	0.023(2)
F10	8*c*	0.6551(4)	0.1611(3)	0.3636(9)	0.028(2)
F11	4*b*	¼	0.4318(3)	0.188(2)	0.036(3)
F12	4*b*	¼	0.6508(2)	0.157(2)	0.018(2)
O1	4*b*	¼	0.2634(3)	0.116(2)	0.021(2)
O2	4*a*	0	0	0.000(2)	0.018(2)

U_{eq} is defined as one third of the trace of the orthogonalized U_{ij} tensor (standard deviations in parentheses).

Table 3: Anisotropic displacement parameters U_{ij} in Å^2 (standard deviations in parentheses).

Atom	U_{11}	U_{22}	U_{33}	U_{23}	U_{13}	U_{12}
Sn1	0.0075(2)	0.0092(2)	0.0075(2)	0.0000(3)	0.0003(3)	−0.0021(2)
Sn2	0.0083(2)	0.0120(2)	0.0058(2)	0.0003(4)	0.0006(3)	0.0041(1)
K1	0.027(1)	0.024(1)	0.016(2)	−0.0013(8)	−0.0050(8)	−0.0103(8)
K2	0.0082(7)	0.0125(7)	0.0158(8)	−0.002(2)	0.003(2)	0.0000(5)
K3	0.0178(7)	0.0236(8)	0.0142(8)	0.000(2)	−0.004(1)	−0.0088(6)
K4	0.023(2)	0.013(2)	0.036(2)	0.012(2)	0	0
K5	0.014(1)	0.018(2)	0.010(2)	−0.001(2)	0	0
K6	0.016(2)	0.016(2)	0.041(2)	0.004(2)	0	0
K7	0.008(2)	0.014(2)	0.014(2)	−0.0002(9)	0	0
F1	0.019(3)	0.038(3)	0.019(3)	−0.016(2)	0.008(2)	−0.015(2)
F2	0.007(2)	0.022(2)	0.030(3)	−0.004(3)	0.005(3)	0.004(2)
F3	0.035(3)	0.016(3)	0.034(3)	0.015(2)	0.008(2)	0.010(2)
F4	0.016(4)	0.030(5)	0.017(3)	0.012(3)	0.005(3)	0.004(4)
F5	0.017(2)	0.029(3)	0.015(2)	−0.003(2)	0.011(2)	−0.005(2)
F6	0.054(5)	0.049(5)	0.039(4)	−0.025(4)	−0.009(4)	0.026(4)
F7	0.017(3)	0.031(3)	0.021(3)	−0.007(2)	0.003(2)	−0.014(2)
F8	0.018(4)	0.015(4)	0.021(3)	0.011(3)	0.001(3)	0.001(3)
F9	0.016(3)	0.024(3)	0.029(3)	−0.011(2)	0.000(2)	−0.008(2)
F10	0.024(4)	0.028(4)	0.033(4)	−0.017(3)	−0.011(3)	0.011(3)
F11	0.030(4)	0.017(4)	0.061(7)	−0.010(4)	0	0
F12	0.012(3)	0.011(3)	0.032(5)	−0.008(4)	0	0
O1	0.005(3)	0.023(4)	0.037(5)	0.003(7)	0	0
O2	0.022(5)	0.019(5)	0.012(4)	0	0	−0.009(4)

Table 4: Interatomic distances in pm (standard deviations in parentheses).

Sn1–O2	194.7(3)	Sn2–O1	195.3(2)		K1–F1	256.4(5)		K2–F12	259.8(2)	
–F7	196.8(5)	–F10	196.4(6)		–F9	273.4(5)		–F3	267.0(6)	
–F1	197.1(5)	–F6	197.5(7)		–F5	277.3(5)		–F7	267.2(5)	
–F9	197.5(4)	–F4	200.1(6)		–F11	280.2(2)		–F2	269.3(4)	
–F5	197.7(4)	–F8	200.1(6)		–F6	281.1(8)		–F8	269.9(6)	
–F3	198.6(5)	–F2	200.3(4)		–O2	286.4(5)		–F4	274.8(7)	
					–F3	320.4(6)		–F1	275.2(5)	
					–F10	336.4(7)		–F5	301.2(6)	
K3–F3	251.9(5)	K4–F7	250.4(5)	2×	K5–F12	261.9(6)		K6–F10	2.692(7)	2×
–F4	274.1(7)	–F12	254(1)		–F4	285.2(7)	2×	–F9	2.717(5)	2×
–F10	279.6(7)	–O1	263.0(7)		–F8	290.5(7)	2×	–F11	3.014(9)	
–F2	282.2(4)	–F8	315.8(7)	2×	–O1	296(2)		–F11	3.020(9)	
–F8	283.2(7)				–F10	298.3(8)	2×	–F6	3.062(8)	2×
–F2	289.8(9)				–O1	301(2)				
–F6	300(1)				–F6	318.2(8)	2×			
–F8	303.9(7)							K7–F5	2.617(4)	2×
–F4	305.6(7)							–F11	2.747(7)	
–F2	307.4(9)							–F7	2.759(6)	2×
								–F12	2.778(6)	
								–F9	2.937(5)	2×

100 detector and an Incoatec microfocus X-ray tube (Incoatec, Geesthacht, Germany) using Mo$K\alpha$ radiation ($\lambda = 71.07$ pm). The measurement was conducted at $T = 183(2)$ K. The intensity data was corrected by multi-scan absorption correction, using SADABS 2014/5. The space groups $Cmc2_1$ (no. 36), *Cmcm* (no. 63), and *Ama*2 (no. 40) were considered for the structure solution (SHELXTL-XT-2014/4) and refinement based on the

Table 5: Bond angles in deg (standard deviations in parentheses).

O2–Sn1–F7	177.4(2)	O2–Sn1–F1	98.3(2)	O1–Sn2–F10	96.1(4)
F1–Sn1–F5	170.4(2)	F7–Sn1–F1	83.2(2)	O1–Sn2–F6	99.0(4)
F9–Sn1–F3	171.1(2)	O2–Sn1–F9	97.4(2)	F10–Sn2–F6	95.8(3)
Ø $_{180}$	**173.0**	F7–Sn1–F9	84.7(2)	O1–Sn2–F4	91.4(4)
		F1–Sn1–F9	91.4(2)	F6–Sn2–F4	90.0(3)
		O2–Sn1–F5	90.8(2)	O1–Sn2–F8	88.4(4)
		F7–Sn1–F5	87.6(2)	F10–Sn2–F8	86.0(3)
F10–Sn2–F4	169.6(3)	F9–Sn1–F5	90.4(2)	F4–Sn2–F8	87.1(2)
F6–Sn2–F8	172.1(4)	O2–Sn1–F3	90.8(2)	F10–Sn2–F2	87.0(3)
O1–Sn2–F2	171.0(3)	F7–Sn1–F3	87.0(2)	F6–Sn2–F2	89.1(3)
Ø $_{180}$	**170.9**	F1–Sn1–F3	90.9(2)	F4–Sn2–F2	84.5(3)
		F5–Sn1–F3	86.0(2)	F8–Sn2–F2	83.3(3)
		Ø $_{90}$	**89.9**	**Ø $_{90}$**	**89.8**

extinction conditions. *Ama*2 (no. 40) was found to be correct. Parameter refinement (full-matrix least-squares against F^2) was carried out with SHELXL-2013 [10, 11] (implemented in the WINGX-2013.3 [12] suite). The anisotropic refinement led to values of 0.0389 and 0.0443 for *R*1 and *wR*2 (all data), respectively. The final solution was checked with PLATON [13] (implemented in the WINGX-2013.3 [12] suite) to ensure that no higher symmetry was overlooked.

Further information on the crystal structure investigation can be obtained from the joint CCDC/FIZ Karlsruhe deposition service on quoting the deposition number CCDC 1956612 for $K_5Sn_2OF_{11}$.

2.3 EDX spectroscopy

The chemical composition was analysed by energy dispersive X-ray spectroscopy (EDX) using a SUPRA™35 scanning electron microscope (SEM, Carl Zeiss, Oberkochen, Germany, field emission) equipped with a Si/Li EDX detector (Oxford Instruments, Abingdon, Great Britain, model 7426).

2.4 Vibrational spectroscopy

A Bruker Alpha-P spectrometer (Bruker, Billerica, USA), equipped with a DTGS detector and a 2×2 mm diamond

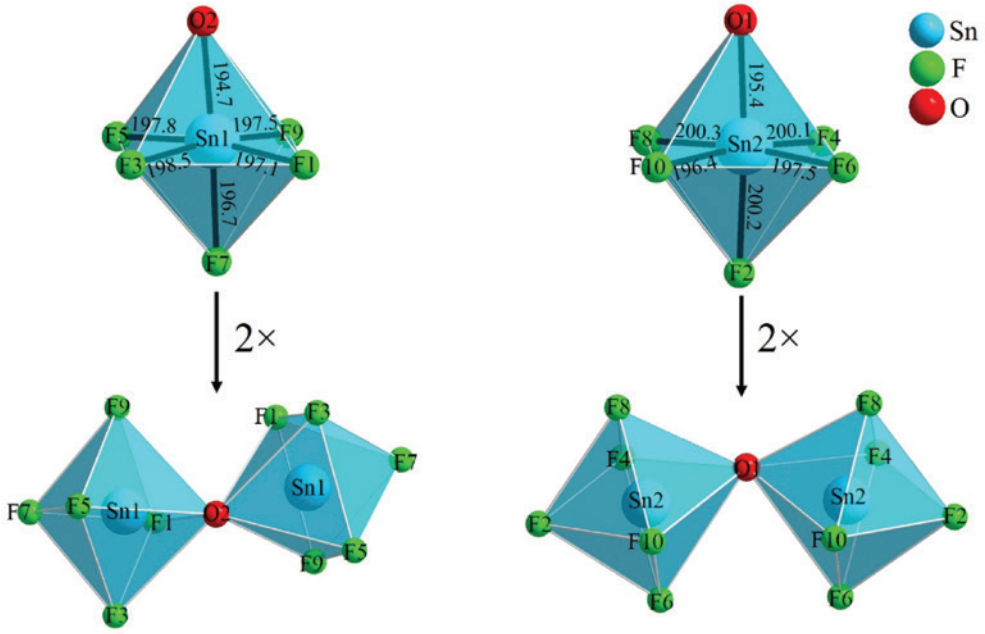

Fig. 2: Octahedral coordination spheres of Sn1 (left, top) and Sn2 (right, top) and the connection of two similar octahedra *via* a bridging oxygen atom to $[Sn_2OF_{10}]^{4-}$ units (bottom).

ATR-crystal, was used for the characterization of $K_5Sn_2OF_{11}$ by FTIR-ATR (Attenuated Total Reflection) spectroscopy. The handling of the data was carried out using the Opus 7.2 software.

3 Results and discussion

3.1 Crystal structure

$K_5Sn_2OF_{11}$ crystallizes in the orthorhombic system in the non-centrosymmetric space group *Ama*2 (no. 40) with cell parameters of $a = 1758.3(2)$, $b = 2452.3(2)$ and $c = 596.7(1)$ pm and a volume of $V = 2.5727(4)$ nm^3. The unit cell is assembled from eight formula units and contains 152 atoms. The asymmetric unit consists of 23 different positions. Sn1, Sn2, K1, K2, K3, and F1 to F10 are located at general positions (Wyckoff sites 8*c*), whereas K4, K5, K6, K7, and O1 are located at special positions on the Wyckoff site 4*b*, as well as F11 and F12. Furthermore, O2 is located on a special position (Wyckoff site 4*a*). The structure was refined as an inversion twin, with a ratio of 0.31(4) to 0.69(4). Details on the structural refinement can be found in Table 1. Important distances, as well as angles, the atomic positions, and anisotropic displacement parameters, are reported in Tables 2–5.

The main structural motifs of $K_5Sn_2OF_{11}$ are two different $[Sn_2OF_{10}]^{4-}$ units. Building unit 1 (BU1, Fig. 2, left) consists of two identical octahedra built up of Sn1 as central cation, which is coordinated by five fluorine atoms (F1, F3, F5, F7, F9) and one oxygen atom (O2). The two octahedra share the bridging oxygen atom (O2) and are tilted (Sn1–O2–Sn1 = 130.04(1)°) and twisted against each other (dihedral angle F5–Sn1–Sn1–F5 ≈ 52°). The second $[Sn_2OF_{10}]^{4-}$ unit (BU2) is built up of two identical $[Sn2OF_5]^{3-}$ octahedra (Fig. 2, right), which share a common corner (O1). These two octahedra are tilted towards each other with an Sn2–O1–Sn2 angle of 141.23(1)°. Within both units (BU1 and BU2), the Sn–F bond lengths vary between 196.4(6) and 200.3(4) pm, while the Sn–O bond lengths are slightly shorter with 194.7(3) and 195.3(2) pm for Sn1–O2 and Sn2–O1, respectively. The more covalent character of the Sn–O bond in comparison to the Sn–F bond may lead to this effect. These two building units are imbedded into a matrix consisting of potassium cations and fluoride anions.

Within the structure, there are seven crystallographically independent potassium positions and two independent fluoride positions. K2, K6, and K7 are eightfold coordinated and K3 is tenfold coordinated solely by fluorine atoms. In comparison, K1 is eightfold coordinated by

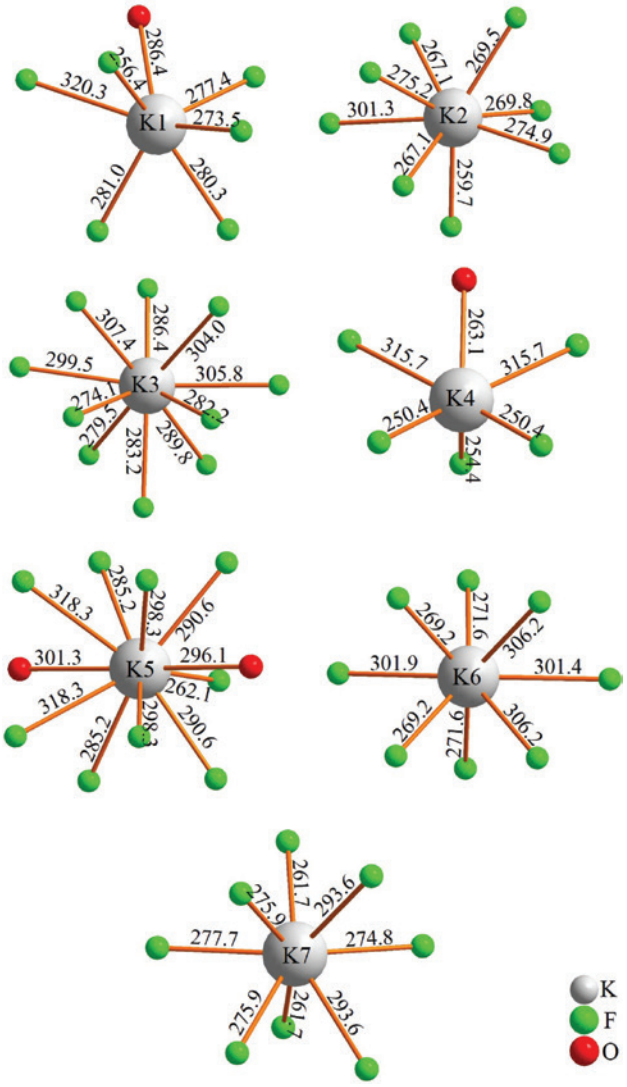

Fig. 3: Coordination spheres of the potassium cations in $K_5Sn_2OF_{11}$ (bond lengths are given in pm).

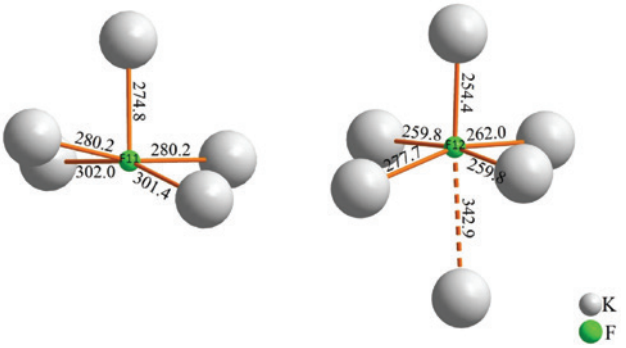

Fig. 4: Coordination spheres of F11 (left) and F12 (right) in the structure of $K_5Sn_2OF_{11}$ (bond lengths are given in pm).

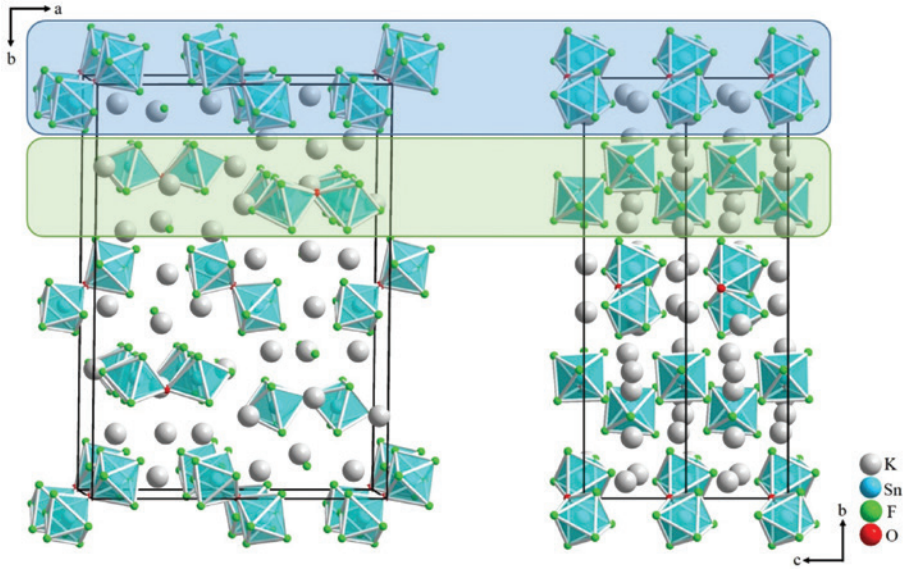

Fig. 5: Unit cell and adjacent octahedra of $K_5Sn_2OF_{11}$ viewed approx. along [001] (left), and a doubled unit cell viewed along [$\bar{1}$00] (right). Layers built up of BU1 are marked in blue; layers consisting of BU2 are marked in green.

Table 6: Values of the charge contributions according to both the bond valence sums (∑V) and the CHARDI (∑Q) concept.

	Sn1	Sn2	K1	K2	K3	K4	K5	K6	K7
BLBS	+4.39	+4.25	+0.89	+1.13	+1.02	+1.07	+0.96	+0.82	+1.03
CHARDI	+3.95	+3.94	+1.11	+0.99	+0.97	+0.97	+1.01	+1.06	+1.05
	F1	**F2**	**F3**	**F4**	**F5**	**F6**	**F7**	**F8**	**F9**
BLBS	−1.05	−1.04	−1.12	−1.07	−1.06	−0.97	−1.25	−1.09	−1.05
CHARDI	−1.01	−1.02	−1.01	−1.05	−1.03	−1.00	−1.20	−1.05	−1.07
	F10	**F11**	**F12**	**O1**	**O2**				
BLBS	−1.08	−0.48	−0.92	−2.22	−2.06				
CHARDI	−1.10	−0.58	−0.85	−1.81	−1.67				

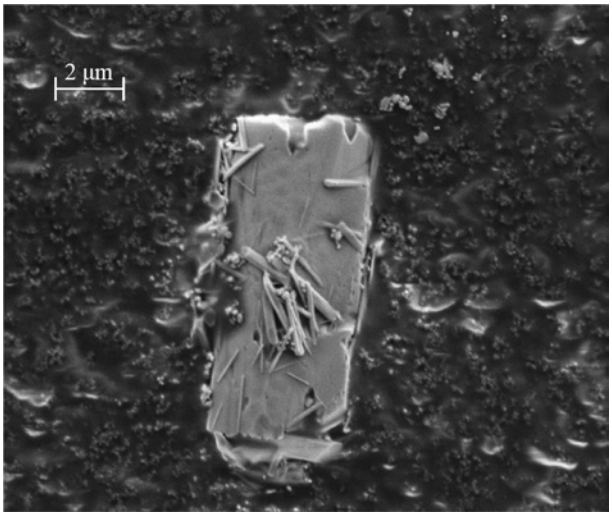

Fig. 6: SEM image of a polycrystalline sample of $K_5Sn_2OF_{11}$.

one oxygen and seven fluorine atoms, K4 sixfold by one oxygen and five fluorine atoms, and K5 11-fold by two oxygen and nine fluorine atoms. The coordination spheres of all potassium cations are depicted in Fig. 3. The K–F bond lengths range from 250.4(5) to 336.4(7) pm and the K–O bond lengths range from 263.0(7) to 301(2) pm.

The atoms F11 and F12 are solely coordinated by potassium cations. In detail, F11 is fivefold coordinated (Fig. 4, left) and F12 exhibits a 5+1 coordination (Fig. 4, right).

A unit cell of the layer-like crystal structure is depicted in Fig. 5 (left). Layers consisting of quasi-isolated BU1 (Fig. 5, marked blue) entities alternate with layers consisting of quasi-isolated BU2 units (Fig. 5, marked green). These layers are stacked along the crystallographic *b* axis and are separated by independent fluorine and potassium

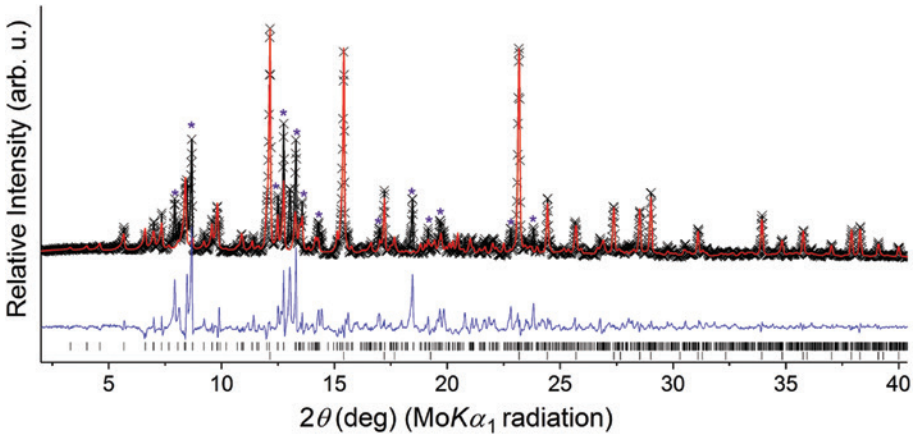

Fig. 7: Rietveld analysis of a PXRD pattern of the synthesized sample. Measured data is plotted as black crosses, the calculated curve in red and the difference curve in blue. Reflection positions originating from $K_5Sn_2OF_{11}$ are shown in black (top tick marks below the difference curve in blue), and the ones originating from SnO_2 are also marked in black (bottom tick marks). Additionally, purple asterisks mark reflections of an unknown side phase.

atoms (Fig. 5, left). Within the layer of the BU1 units, the building blocks (BU1) are tilted alternatingly left and right along the *a* axis. In contrast, the BU2 units point alternatingly up- or downwards within their layer. Within this set-up, every second layer made up by BU1 or BU2, respectively, is shifted by half a unit cell along the *c* axis (Fig. 5, right).

The structure model was confirmed by bond-length/bond-strength (BLBS) [14, 15] and charge distribution (CHARDI) [16] calculations (Table 6). The highest discrepancy is found at F11 with −0.48 and −0.58 for BLBS and CHARDI, respectively. This low value can likely be attributed to the uncommon pyramidal coordination of F11 (Fig. 4, left).

The chemical composition of $K_5Sn_2OF_{11}$ regarding the cations was confirmed by EDX spectroscopy to be 5:1.8(4) (potassium to tin). An SEM image of a polycrystalline part of the sample is depicted in (Fig. 6).

Powder XRD analysis *via* the Rietveld technique showed that $K_5Sn_2OF_{11}$ could be synthesized as the main component (68 wt.-%), but not phase pure (Fig. 7). Along with an unknown side phase (purple asterisks, Fig. 7), SnO_2 could be identified as residual starting material (32 wt.-%, black tickmarks, bottom, Fig. 7). The lattice parameters determined by the Rietveld technique are listed in Table 1. They cannot be compared directly with the ones obtained by the single-crystal measurements, as the powder data were recorded at room temperature, whereas the single-crystal data were recorded at $T = 183(2)$ K.

The substance was further characterized by infrared spectroscopy (Fig. 8, black line). The spectrum shows an intense absorption band at approx. 518 cm^{-1}, which has also been described for $K_4Sn_2OF_{10}$ (strong band at 530 cm^{-1}) [8]. Two sharp maxima are located at approx. 608 cm^{-1} and 803 cm^{-1}, which are also in accordance with $K_4Sn_2OF_{10}$ (medium strong band at 610 cm^{-1}; medium strong band at 845 cm^{-1}) [8]. Two bands at 518 cm^{-1} and 608 cm^{-1} are observed for SnO_2 (Fig. 8, red line) and two broad absorption bands at approx. 1500 cm^{-1} and 3300 cm^{-1} can likely be attributed to water, which starts to intercalate into the structure, as the substance seems to be sensitive to moisture.

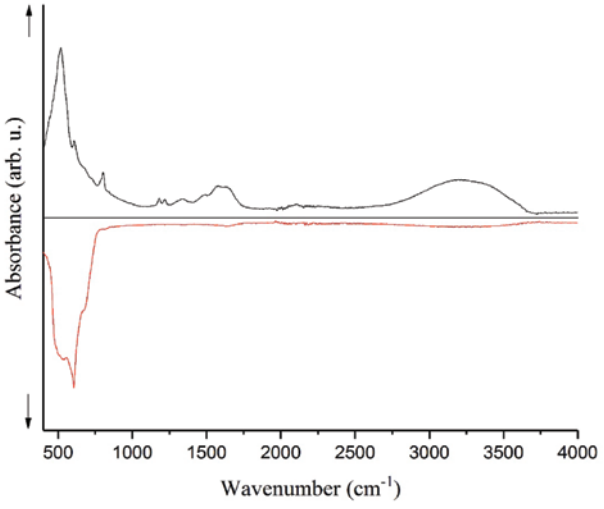

Fig. 8: FT-IR spectrum in the range of 400 to 4000 cm^{-1}. The black line shows the spectrum of the sample; the red line gives the spectrum of SnO_2, which is present as a residual starting material.

4 Conclusion

$K_5Sn_2OF_{11}$ was successfully characterized by means of single-crystal and powder X-ray diffraction data. It exhibits two different kinds of dinuclear $[Sn_2OF_{11}]^{5-}$ units, which are built up of corner-sharing $[SnOF_5]^{3-}$ octahedra. These structural units are imbedded into a matrix consisting of potassium cations and fluoride anions. BLBS and CHARDI calculations confirmed the structural model. As the structure crystallizes in a non-centrosymmetric space group, it would be quite interesting to analyze the NLO properties of a phase-pure sample of $K_5Sn_2OF_{11}$. Additionally, the $[Sn_2OF_{11}]^{5-}$ units might qualify for a partial substitution with Mn^{4+} to yield a red luminescent material as described for other oxidofluoridometallates like K_3WOF_7 [17].

Acknowledgment: We want to express our gratitude to Assoc.-Prof. Dr. Gunter Heymann for the collection of the single-crystal data and to Dr. Klaus Wurst for the help with the crystal structure refinement. We also want to thank Christian Koch for the EDX and SEM measurements.

References

[1] M. Leblanc, V. Maisonneuve, A. Tressaud, *Chem. Rev.* **2015**, *115*, 1191–1254.
[2] C. Stoll, M. Seibald, D. Baumann, H. Huppertz, *Eur. J. Inorg. Chem.* **2019**, *29*, 3383–3388.
[3] P.-Y. Chiang, T.-W. Lin, J.-H. Dai, B.-C. Chang, K.-H. Lii, *Inorg. Chem.* **2007**, *46*, 3619–3622.
[4] M. Mann, J. Kolis, *Acta Crystallogr.* **2009**, *C65*, i17–19.
[5] D. Santamaría-Pérez, A. Vegas, U. Müller, *Solid State Sci.* **2005**, *7*, 479–485.
[6] J.-H. Chang, J. Köhler, *Z. Kristallogr. NCS* **1999**, *214*, 147–148.
[7] B. Darriet, J. Galy, *Acta Crystallogr.* **1977**, *B33*, 1489–1492.
[8] L. Kolditz, H. Preiss, *Z. Anorg. Allg. Chem.* **1963**, *325*, 263–274.
[9] R. Pöttgen, T. Gulden, A. Simon, *GIT Labor-Fachz.* **1999**, *43*, 133–136.
[10] G. M. Sheldrick, *Acta Crystallogr.* **2008**, *A64*, 112–122.
[11] G. M. Sheldrick, *Acta Crystallogr.* **2015**, *C71*, 3–8.
[12] L. J. Farrugia, *J. Appl. Crystallogr.* **2012**, *45*, 849–854.
[13] A. L. Spek, *Acta Crystallogr.* **2009**, *D65*, 148–155.
[14] N. E. Brese, M. O'Keeffe, *Acta Crystallogr.* **1991**, *B47*, 192–197.
[15] I. D. Brown, D. Altermatt, *Acta Crystallogr.* **1985**, *B41*, 244–247.
[16] R. Hoppe, S. Voigt, H. Glaum, J. Kissel, H. P. Müller, K. Bernet, *J. Less-Common Met.* **1989**, *156*, 105–122.
[17] C. Stoll, G. Heymann, M. Seibald, D. Baumann, H. Huppertz, *J. Fluorine Chem.* **2019**, *226*, 109356.